



HAL
open science

Supramolecular carbohydrate-based hydrogels from oxidative hydroxylation of amphiphilic β -C-glycosylbarbiturates and α -glucosidase-induced hydrogelation

Shun Yao, Robin Brahmi, Anaïs Bouschon, Jing Chen, Sami Halila

► To cite this version:

Shun Yao, Robin Brahmi, Anaïs Bouschon, Jing Chen, Sami Halila. Supramolecular carbohydrate-based hydrogels from oxidative hydroxylation of amphiphilic β -C-glycosylbarbiturates and α -glucosidase-induced hydrogelation. *Green Chemistry*, 2022, 25 (1), pp.330-335. 10.1039/D2GC04180D . hal-03920384

HAL Id: hal-03920384

<https://cnrs.hal.science/hal-03920384>

Submitted on 3 Jan 2023

HAL is a multi-disciplinary open access archive for the deposit and dissemination of scientific research documents, whether they are published or not. The documents may come from teaching and research institutions in France or abroad, or from public or private research centers.

L'archive ouverte pluridisciplinaire **HAL**, est destinée au dépôt et à la diffusion de documents scientifiques de niveau recherche, publiés ou non, émanant des établissements d'enseignement et de recherche français ou étrangers, des laboratoires publics ou privés.

Supramolecular carbohydrate-based hydrogels from oxidative hydroxylation of amphiphilic β -C-glycosylbarbiturates and α -glucosidase-induced hydrogelation

Shun Yao,^a Robin Brahmi,^a Anaïs Bouschon,^a Jing Chen,^b Sami Halila^{a,*}

We describe an ecofriendly two-step synthesis of glycoamphiphiles, capable of hierarchical self-assembly towards supramolecular hydrogels, and consisting in Knoevenagel condensation of barbituric derivatives onto biobased carbohydrates (glucose and maltose) and selective H_2O_2 -mediated oxidative hydroxylation of the barbiturate in water. By playing on the molecular design of glycostructures and on hydrophilic/hydrophobic balance, various glyco-nanostructures (ribbons, tapes, vesicles, helices, fibers) have been created *via* supramolecular self-assembly. In addition, we found that one water-soluble glycoamphiphile underwent sol-to-gel phase transition upon the addition of α -glucosidase as a result of the hydrolysis of the non reducing-end glucose in maltose moiety.

Introduction

Glycoamphiphiles are basically defined as a hydrophilic carbohydrate moiety covalently bound *via* a glycosidic linkage to a hydrophobic building block. In Nature, such amphiphilic species exist as glycolipids (glycosphingolipids, glycosylphosphatidylinositols, lipopolysaccharides, etc.) that are essential components of cell membranes and mediate diverse biological and pathological processes such as cell growth, fertility, immunity, metastasis, and viral and microbial invasion.^{1,2} On the other hand, because of their self-assembling properties, their renewable raw materials, low toxicity and high biodegradability, glycoamphiphiles found many applications in a huge variety of fields, from agriculture to biomedical applications.^{3,4} For instance, alkylpolyglucoside is used as a foaming agent, emulsifier, pharmaceutical granulating agent and cosmetic surfactant.⁵ Besides, glycoamphiphiles display advanced functions such as liquid crystals properties or self-assembly properties into various nanostructures ranging from micelles, vesicles and fibers in solution.⁶⁻⁸ A milestone was reached when we demonstrated that amphiphilic carbohydrate-based block copolymers could self-organized into periodic thin-films nanostructures of sub-10 nm resolution.⁹⁻¹¹ In addition, glycoamphiphiles or glyco-hydrogelators are known to form supramolecular hydrogels resulting from the three-dimensional network of interpreted self-assembled nanofibers.¹²⁻¹⁴ Supramolecular hydrogels have gained tremendous attention in the development of soft materials with applications as drug releasing matrices, tissue engineering, removal of pollutants, sensors or template for nanostructured materials, etc...¹⁵⁻¹⁷ Glyco-hydrogelators are mainly achieved through a multi-step synthesis including protection/functionalization/deprotection reactions in toxic and unsustainable solvents that is non economical and ecofriendly strategy and remains a time-consuming and labor-intensive process.¹²⁻¹⁴

Very recently, we tackled these problematics by reporting an efficient and versatile green synthetic access to glyco-hydrogelators through the Knoevenagel condensation in water of *N,N'*-substituted barbituric acids with protecting group-free carbohydrates.¹⁸ The resulting sodium salt of *N*-monosubstituted β -C-glycosylbarbiturates led to entangled nanostructured hydrogels either in strong acidic conditions or either by adding calcium ions at neutral pH (Fig. 1). Because of hydrogelation conditions that are inconsistent with biological applications, we investigated, once again, a sustainable chemical way to perform hydrogelation of β -C-glycosylbarbiturates at neutral pH and without adding divalent metal ions.

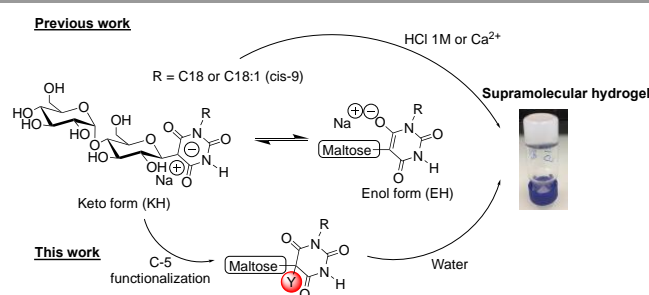


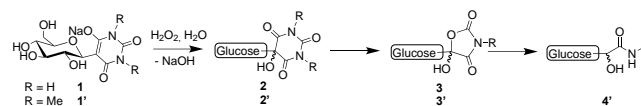
Fig. 1 Structures and conditions of hydrogelation of sodium salt of amphiphilic β -C-glycosylbarbiturates

Starting from the observation that the exclusive presence of the keto tautomer form (KH) of barbiturates, that could be in equilibrium with the enol tautomer form (EH), is mandatory to promote hydrogelation, we decided, in this paper, to investigate the post-functionalization at the C-5 position of the barbituric moiety of the glycoamphiphiles, thus definitively blocking the KH form (Fig. 1). A survey of the literature indicated that reactions of i) bromination,¹⁹ ii) alkylation,^{20,21} iii) hydroxy methylation,²² iv) malonyl peroxides-mediated oxidation,²³ and v) oxidative hydroxylation could be envisioned. Keeping in mind that green chemistry approaches should be favored, we took the route of oxidative hydroxylation²⁴ that occurs in water.

Therefore, herein, we describe the selective oxidative hydroxylation of a series of amphiphilic *N*-monosubstituted β -C-glycosylbarbiturates as well as an investigation of their hydrogelation properties in pure water.

Results and discussion

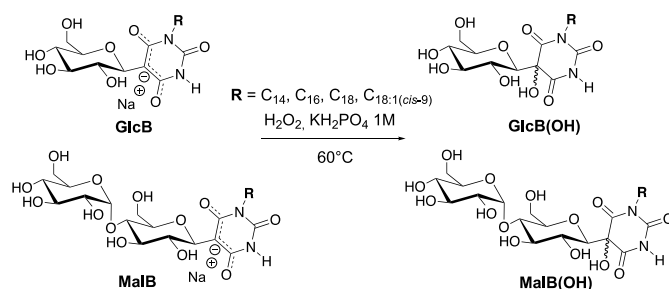
Our first attempts of selective oxidative hydroxylation at C-5 position of the barbiturate ring were done with model substrates, such as β -C-glucosylbarbiturate **1** and *N,N*-dimethyl β -C-glucosylbarbiturate **1'**, that were easily synthesized and isolated from the aqueous reaction by precipitation into a mixture of EtOH/EtOAc (2:6; v/v) with 96 % and 98 % yields, respectively (Scheme 1).²⁵ A previous work from L'Oréal group reported that H₂O₂-mediated oxidative hydroxylation of **1'** in water led in a one-pot procedure to β -methylamide C-glucoside derivative **4'** involving the release of NaOH in the mechanism pathway.²⁶



Scheme 1 H₂O₂-mediated oxidative hydroxylation of β -C-glucosylbarbiturate **1** and **1'**.

Moreover, a patent from the previous authors showed that the oxazolidine-2,4-dione intermediates **3** and **3'** could be favoured by controlling the reaction time or by using oxone[®] as oxidizing reagent during 16 h.²⁷ For the latter, by reducing the reaction time from 16 to 2 h, the C-5 hydroxyl derivative **2'** have been obtained in 71% yield. And the compound **2** was not described. In this work, H₂O₂ was preferred because is a very mild oxidant, relatively cheap and produces only water as by-product, thus benefiting both the economic and green chemistry viewpoints. Since the basic conditions of H₂O₂-mediated oxidative hydroxylation led preferentially to rearrangements, we treated **1'** with 2 equivalents of KH₂PO₄ 1M in order to control the pH (between 7 and 8) during the reaction. In spite of these precautions, we rapidly obtained a mixture of oxazolidinone **2'** and C-5 hydroxyl **3'** derivatives according to mass spectrometry analysis (data not shown). However, the same experimental conditions applied to **1** led to **2** in a satisfactory yield of 66%. This result highlights that *N*-H groups kinetically disfavors the rearrangement pathway, thereby allowing control of the oxidative hydroxylation at the C-5 position of the barbituric acid.

As previously mentioned, we already demonstrated that **MalB-3** and **MalB-4** (Fig. 1), that are featured by a maltose disaccharide linked through a *N*-monosubstituted barbiturate to a C18 saturated aliphatic chain and C18 mono-unsaturated C18:1 (*cis*-9) chain, respectively, were able to hierarchically self-assemble into supramolecular hydrogels in strong acidic conditions or by adding calcium ions.¹⁸ We found, with others,²⁸⁻³⁰ that the hydrophobic-hydrophilic balance is a determinant parameter for exhibiting hydrogelation and since oxidative hydroxylation brings an additional hydroxyl function, we decided to screen a library of synthetic amphiphilic β -C-glycosylbarbiturates **GlcB(OH)** and **MalB(OH)** towards their hydrogelation abilities (Scheme 2).



Scheme 2 H₂O₂-mediated oxidative hydroxylation of sodium salt of amphiphilic β -C-glycosylbarbiturate **GlcB** and **MalB** towards neutral amphiphilic hydroxylated β -C-glycosylbarbiturate **GlcB(OH)** and **MalB(OH)**.

Table 1 Yields of oxidative hydroxylation affording amphiphilic β -C-glycosylbarbiturate **GlcB(OH)** and **MalB(OH)**.

Glucose	R	Maltose	% yield ^a
GlcB(OH)	1	1	58
	2	2	64
	3	3	56
	4	4	63
		MalB(OH)	
	C14		72
	C16		54
	C18		67
	C18:1(<i>cis</i> -9)		63

^a Conversion in isolated product.

Briefly, the synthesis of **GlcB** and **MalB** were performed through Knoevenagel condensation in water by reacting chemo-selectively *N,N'*-alkyl barbituric acid derivatives into the reducing-end anomeric position of unprotected **Glc** and **Mal**, as already reported.¹⁸ Next, H₂O₂-mediated oxidative hydroxylation of **GlcB** and **MalB** in water led successfully to **GlcB(OH)** and **MalB(OH)**, respectively, with moderate to good yields (54 - 72%) as shown in Table 1. While thin-layer chromatography analyses indicated an almost complete reaction, a chromatographic separation step was required, lowering the yields in isolated products. All the structures were characterized and confirmed by high resolution mass spectrometry, NMR, FTIR and UV-visible spectroscopy (See ESI[†] and Fig. S1-S8). The formation of 5,5-disubstituted barbiturates induces significant upfield shift of the *H*-anomeric involved in β -C-glycoside formation that appears as a clean doublet at 4.5 ppm in **GlcB** and **MalB** (Fig. S9[†]).¹⁸ The keto tautomer form for the series

of **GlcB(OH)** and **MalB(OH)** was also confirmed by UV-visible spectroscopy with an expected λ_{\max} around 230 nm and nothing at 262 nm, such as for **GlcB-1**, which is the signing of the enol tautomer form (Fig. 2).¹⁸

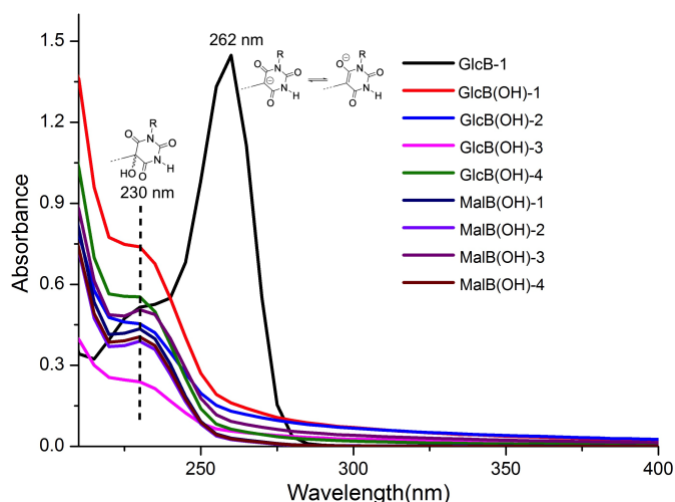


Fig. 2 UV spectrum of **GlcB(OH)** and **MalB(OH)** in water showing λ_{\max} at 230 nm corresponding to keto tautomer forms and of **GlcB-1** showing λ_{\max} at 262 nm corresponding to a mixture of enol and keto tautomer forms.

To investigate the self-assembling properties of **GlcB(OH)** and **MalB(OH)**, tube-inversion experiments were realized, that involved cooling to induce gelation (self-assembly) after dissolution into aqueous solution *via* heating at 80°C (Table 2). In contrast to **GlcB** samples that didn't dissolved into water even after heating, **GlcB(OH)** samples dissolved upon heating and more importantly slightly opaque hydrogels were formed after cooling-down at room temperature (rt) with a minimal gelation weight concentration (MGC) of 2 wt% for **GlcB(OH)-2**, and 3 wt% for **GlcB(OH)-3** and **GlcB(OH)-4**. **GlcB(OH)-1** dissolved into hot water and upon cooling formed sedimented large spherical aggregates and could not be considered as hydrogel. For **GlcB(OH)-4**, the formation of the hydrogel occurred after 3 days at rest, highlighting particularly low self-assembly kinetics and aging helped for improving packing over time. In summary, these results clearly indicated that the additional hydroxyl function changed dramatically the solubility parameter in pure water and induced hierarchical self-assembly into supramolecular hydrogels. For **MalB(OH)** samples, opaque and transparent hydrogels were only observed for **MalB(OH)-3** at 4 wt% and **MalB(OH)-4** at 5 wt%, respectively. The obtention of a stable transparent gel for **MalB(OH)-4** compared to **MalB(OH)-3** reveals the formation of thinner aggregates that are shorter than the visible wavelength region. Decreasing the aliphatic chain from C18 (**MalB(OH)-3**) to C16 (**MalB(OH)-2**) and C14 (**MalB(OH)-1**) resulted in a full solubility in water. While **MalB(OH)-3** is stable at room temperature for several months, **MalB(OH)-4** becomes liquid after 1 day at rt. The hydrogels were all thermoreversible, as confirmed by alternating heating (solution) and cooling (gel) cycles, that is one of characteristics of supramolecular hydrogels owing to the nature of weak interconnected bonds. Gel-to-sol transition (T_{gel}) of the hydrogel at MGC was investigated by differential scanning calorimetry (DSC) which showed an endothermic peak at 64, 61, 42, 38°C for **GlcB(OH)-2** to **-4**, respectively and 38°C for both **MalB(OH)-3** and **-4**, supporting the disruption of the gel phase (Table 2).

Table 2 Pictures of the hydrogels and properties in water of **GlcB(OH)** and **MalB(OH)**.

GlcB(OH)				MalB(OH)			
1	2	3	4	1	2	3	4
P	G2 _o	G3 _o	G3 _o	S	S	G4 _o	G5 _T
				-	-		
T_{gel} (°C)	64	61	42			38	38

G: stable gel at room temperature, the numbers close to G indicate the MGCs; P: precipitation; S: soluble; O: opaque; T: transparent. T_{gel} represents gel-to-sol transition temperature of hydrogels at MGCs obtained from DSC.

To get a deeper insight into the morphology of self-assembled glyco-hydrogels, transmission electron microscopy observations were performed. As shown in Fig. 3, various well-structured nanoscale architectures entrapping solvent water molecules in the 3-D network were observed and featured by carbohydrates exposed at the periphery. **GlcB(OH)-2** self-assembled into ribbons constituted of fine fibrils (white arrow in Fig. 3A) across their width, while **GlcB(OH)-3** revealed uneven giant multilamellar vesicles ranging from 0,3 to 1 μm in diameter (Fig. 3B) as already observed for phospholipids.³¹ For the latter, the matrix of the hydrogel seems to be formed by the closely packed structures of multilamellar vesicles as already reported in our recent publication.¹⁸ For **GlcB(OH)-4**, TEM showed micrometers long semi-rigid helical nanofibers with a uniform lateral diameter (17 ± 1 nm) close to the lateral arrangement of four **GlcB(OH)-4** molecules (Fig. 3C). **MalB(OH)-3** displayed a plate-like morphology of about hundred nanometers in diameter, (Fig. 3D)³² while **MalB(OH)-4** self-assembled into $5 \pm 0,5$ nm-wide and several micrometer-long tortuous wormlike cylinders consisting with the model of bilayer structures of interdigitated oleyl (C18:1(*cis*-9)) chains (Fig. 3E), that physically entangled into a network that forms the hydrogel matrix. These small wormlike aggregate dimensions confirmed our previous assumption related to the transparency of the hydrogel.

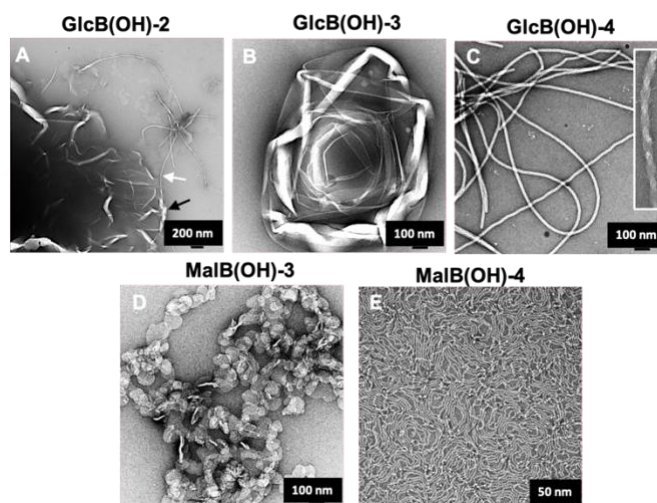


Fig. 3 TEM image of nanostructures of hydrogels formed with **GlcB(OH)-2** (A), **GlcB(OH)-3** (B), **GlcB(OH)-4** including a rectangle zoom (C), **MalB(OH)-4** (D) and **MalB(OH)-5** (E).

If the control of noncovalent interactions with DNA, peptides or phospholipids is well mastered, the known difficulties in controlling the precise structures of carbohydrate-based amphiphiles are closely related the stereochemistry of carbohydrates that greatly impact hydroxyl-based hydrogen bonding (carbohydrate-carbohydrate interactions or CCIs) along with steric effects. However, it is well-established that the self-assembly process is roughly governed by geometrical constraints impacting the surface curvature, of individual uncharged amphiphile molecules (packing parameter),³³ in addition to the attractive hydrophobic interactions between the lipophilic segments and repulsive steric interactions between the hydrophilic headgroups.^{34,35} The different morphologies observed between **GlcB(OH)-3** vs. **MalB(OH)-3** and **GlcB(OH)-4** vs. **MalB(OH)-4** are undoubtedly attributed to molecular geometric considerations and subsequent molecular packing, since Mal disaccharide possesses one additional bulky glucose unit compared to Glc monosaccharide. Moreover, from dissipative particle dynamics simulations with amphiphilic carbohydrate-based metallacycles, G. Chen and coll.³⁶ revealed that a disaccharide displays stronger CCIs than a monosaccharide by four times, driving the self-assembly along the CCIs direction. Therefore, beside the simple molecular geometric considerations, the nature of the carbohydrate headgroup plays also an important role in driving hierarchical self-assembly towards diversiform glyco-nanostructures. Likewise, the morphologies drastically changed from stearyl-containing glycoamphiphiles (**GlcB(OH)-3** or **MalB(OH)-3**) to the counterpart monounsaturated oleyl-containing glycoamphiphiles (**GlcB(OH)-4** or **MalB(OH)-4**) only differing in the absence or presence of a *cis* double bond in the middle of the alkyl chain moiety. Once again, the intermolecular packing plays a significant role because one can expect that oleyl chains, due to the higher chain mobility ($T_m = 13^\circ\text{C}$) than stearyl chain ($T_m = 69^\circ\text{C}$) at RT, will form a tighter intermolecular packing promoting low mean-curvature aggregates such as fiber- or worm-like nanostructures.³⁷ After analyzing individually all the morphologies from the series of **GlcB(OH)-2** to **4**, that varies slightly of two C-C bonds in the hydrophobic chain length, it seems difficult to get direct relationships with the molecular packing parameters. Above all, our results emphasize that HLB still plays a major role for driving their self-assembly behavior regardless of the discrete molecular architectures.

Carbohydrate-based hydrogelators have found many applications in the biomedical field. For instance, supramolecular glyco-hydrogels exhibited inhibition towards biofilm formation and bacterial growth of *P. aeruginosa*,³⁸ served as biomimetic scaffolds for cell growth and adhesion,^{39,40} promoted wound healing,⁴¹ and selectively inhibited cancer cells.⁴² For the latter, Pashkuleva et al.⁴³⁻⁴⁵ originally proposed a simple *N*-Fmoc glucoamine-6-phosphate derivative as a precursor of self-assembly and hydrogelation triggered by the overexpressed alkaline phosphatase-catalyzed dephosphorylation and produced by osteosarcoma cell line. This

innovative supramolecular-based therapeutic axis stems from pioneering works of Bing Xu's group with peptide-based hydrogelator precursors and it is commonly called "Enzyme-Instructed Self-Assembly" or EISA.^{46,47}

By carefully studying the gelation tests of our amphiphilic β -C-glycosylbarbiturates, we identified a potential precursor of hydrogelation that could be induced by the action of α -glucosidases. Indeed, while we demonstrated that **MalB(OH)-2** is fully soluble in water, the monosaccharide analogue **GlcB(OH)-2** formed an opaque hydrogel with a MGC of 2 wt%. So, we evaluated **MalB(OH)-2** as a precursor to turn into a hydrogelator, **GlcB(OH)-2**, upon *Aspergillus niger* amyloglucosidase-catalyzed non-reducing D-glucosyl residue hydrolysis. We started our study by using 3 wt% of **MalB(OH)-2** that should result in 2,3 wt% of **GlcB(OH)-2** if the hydrolysis is total, therefore slightly above MGC. After overnight of enzymatic hydrolysis at 45°C, we were pleased to see that the clear solution turned into an opaque gel. TEM images revealed uniform self-assembled nanofibers (Fig. 4) that differ from the expected ribbons for **GlcB(OH)-2** (Fig. 3A). In addition, if the weight concentration is divided by 5 to reach 0.6 wt% of **MalB(OH)-2**, the α -glucosidase-induced gelation of the resulting **GlcB(OH)-2** occurred and at theoretically 0.46 wt%, which is much lower than MGC. These results pointed out that nanostructure morphologies resulting from self-assembled hydrogelators are clearly dictated by kinetics of supramolecular polymerization (production rate of the hydrogelator) and not only by the tridimensional structure of hydrogelators.⁴⁸ This work reports for the first time the use of α -glucosidase for sol-to-gel phase transition while it was only used for gel-to-sol phase transition.⁴⁹

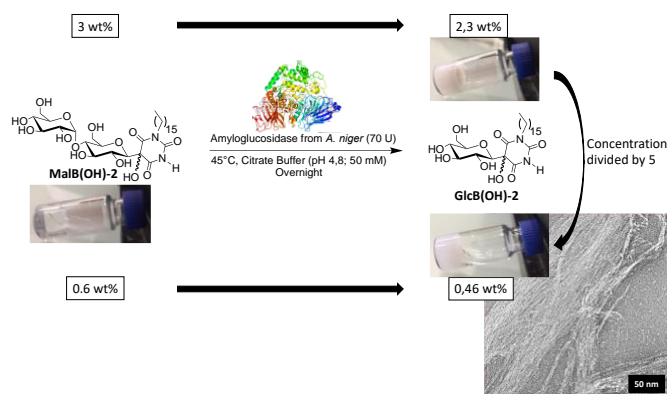


Fig. 4 A. *niger* amyloglucosidase-catalyzed glucosyl residue hydrolysis of **MalB(OH)-2** at 3 and 0,6 wt% into **GlcB(OH)-2** hydrogelator with hydrogel pictures and TEM image of fibrillar glyco-nanostructures.

The *in-vivo* preparation of self-assembled hydrogelators for selective inhibition of cancer cells by taking advantage of overexpressed endogenous enzymes could be envisioned for treating pancreatic cancer, a devastating gastrointestinal cancer, since a recent study demonstrated that an elevated level of lysosomal acid α -glucosidase occurred in response to gemcitabine treatment, an anticancer nucleoside.⁵⁰

Conclusions

In conclusion, following our observation from a previous study that sodium salt of glycosylbarbiturate hydrogelators were effective if the keto form of barbiturate is predominant, we successfully developed a green chemistry derivatization to stabilize the keto form through H_2O_2 -mediated oxidative hydroxylation of the barbiturate ring in water. Thus, we synthesized a series of hydroxylated glycosylbarbiturates and found hydrogelators enabling the supramolecular gelation of water at neutral pH and without the need of strong acid or divalent cations such as for sodium salt of glycosylbarbiturates. Glucose and maltose-based hydrogelators have been discovered resulting in various self-assembled glyco-nanostructures due to their different intermolecular interaction and packing parameters. And in the context of EISA, we showed that α -glucosidase could trigger the formation of supramolecular nanofibers to result in hydrogels and even at a concentration below the minimal concentration of gelation. Indeed, a maltose-based precursor was hydrolyzed into a glucose-based hydrogelator with the use of *Aspergillus niger* amyloglucosidase. Since EISA found relevant applications in cancer therapy by selectively generating *in situ* self-assembled nanostructures or at the periphery of cancer cells, it can be anticipated that these C-glycosylbarbiturates have promising applications in medicine.

Acknowledgements

We are grateful for financial support from CNRS, Université Grenoble Alpes, LabEx ARCANE and CBH-EUR-GS (ANR-17-EURE-0003), the Glyco@Alps program (ANR-15-IDEX-02), Institut Carnot PolyNat (No. 16-CARN-025-01), National Natural Science Foundation of China (51803227), S&T Innovation 2025 Major Special Program of Ningbo (2019B10063), CAS President's International Fellowship for Visiting Scientists (2019VBA0016). All authors acknowledge J. L. Putaux for his help in TEM images

and NanoBio-ICMG Platform (UAR 2607, Grenoble) for granting access to the electron microscopy, NMR and mass spectrometry facilities. S.Y. thanks the China Scholarship Council (CSC) for his scholarship support (201908320428).

References

- 1 B. L. Stocker and M. S. M. Timmer, *ChemBioChem*, 2013, **14**, 1164–1184.
- 2 B. Kalisch, P. Doermann and G. Hoelzl, *Subcell. Biochem.*, 2016, **86**, 51–83.
- 3 B. N. Paulino, M. G. Pessoa, M. C. R. Mano, G. Molina, I. A. Neri-Numa and G. M. Pastore, *Appl. Microbiol. Biotechnol.*, 2016, **100**, 10265–10293.
- 4 I. Mnif and D. Ghribi, *J. Sci. Food Agric.*, 2016, **96**, 4310–4320.
- 5 B. Gutsche and A. Behler, in *Handbook of Detergents, Part F: Production*, ed. U. Zoller and P. Sosis, CRC Press, Boca Raton, FL, 2008, pp. 239–246.
- 6 A. Brito, S. Kassem, R. L. Reis, R. V. Ulijn, R. A. Pires and I. Pashkuleva, *Chem*, 2021, **7**, 2943–2964.
- 7 S. de Medeiros Modolon, I. Otsuka, S. Fort, E. Minatti, R. Borsali and S. Halila, *Biomacromolecules*, 2012, **13**, 1129–1135.
- 8 H. Li, M. Mumtaz, T. Isono, T. Satoh, W.-C. Chen and R. Borsali, *Polym. J.*, 2022, **54**, 455–464.
- 9 K. Aissou, I. Otsuka, C. Rochas, S. Fort, S. Halila and R. Borsali, *Langmuir*, 2011, **27**, 4098–4103.
- 10 J. D. Cushen, I. Otsuka, C. M. Bates, S. Halila, S. Fort, C. Rochas, J. A. Easley, E. L. Rausch, A. Thio, R. Borsali, C. Grant Willson and C. J. Ellison, *ACS Nano*, 2012, **6**, 3424–3433.
- 11 Y. Sakai-Otsuka, S. Zaiocz, I. Otsuka, S. Halila, P. Rannou and Redouane Borsali, *Macromolecules*, 2017, **50**, 3365–3376.
- 12 W. Wang, H. Wang, C. Ren, J. Wang, M. Tan, J. Shen, Z. Yang, P. G. Wang and L. Wang, *Carbohydr. Res.*, 2011, **346**, 1013–1017.
- 13 T. Tsuzuki, M. Kabumoto, H. Arakawa and M. Ikeda, *Org. Biomol. Chem.*, 2017, **15**, 4595–4600.
- 14 M. J. Clemente, P. Romero, J. L. Serrano, J. Fitremann and L. Oriol, *Chem. Mater.*, 2012, **24**, 3847–3858.
- 15 J.Y.C. Lim, Q. Lin, K. Xue and X.J. Loh, *Mater. Today Adv.*, 2019, **3**, 100021.
- 16 A. R. Hirst, B. Escuder, J. F. Miravet and D. K. Smith, *Angew. Chem., Int. Ed.*, 2008, **47**, 8002–8018.
- 17 S. Datta and S. Bhattacharya, *Chem. Soc. Rev.*, 2015, **44**, 5596–5637.
- 18 S. Yao, R. Brahmī, F. Portier, J.-L. Putaux, J. Chen and S. Halila, *Chem. Eur. J.*, 2021, **27**, 16716–16721.
- 19 A. Faust, B. Waschkau, J. Waldeck, C. Hötke, H.-J. Breyholz, S. Wagner, K. Kopka, W. Heindel, M. Scäfers and C. Bremer, *Bioconjugate Chem.*, 2008, **19**, 1001–1008.
- 20 G. Wulff and G. Clarkson, *Carbohydr. Res.*, 1994, **257**, 81–95.
- 21 F. Portier, A. Imbert and S. Halila, *Bioconjugate Chem.*, 2019, **30**, 647–656.
- 22 H. Böhme and H. P. Teltz, *Arch. Pharm.*, 1955, **288**, 349–352.
- 23 A. O. Terent'ev, V. A. Vil, E. S. Gorlov, O. N. Rusina, A. A. Korlyukov, G. I. Nikishin W. Adam, *ChemistrySelect*, 2017, **2**, 3334–3341.
- 24 W. Stadlbauer and T. Kappe, *Monatsh. Chem.*, 1985, **116**, 1005–1015.
- 25 M. Bueno Martinez, F. Zamora Mata, A. Munoz Ruiz and J. A. Galbis Perez, *Carbohydr. Res.*, 1990, **199**, 235–238.
- 26 M.-C. Frantz, S. Dropsit-Montover, F. Pic, A. Prévot-Guéguiniat, C. Aracil, Y. Ding, M. Lima, F. Alvarez, S. Ramos, L. Mao, L. Lu, J. Xu, X. Marat and M. Dalko-Csiba, *Org. Lett.*, 2019, **21**, 2684–2687.
- 27 M. Dalko, A. Prevot-Gueguiniat, M.-C. Frantz and S. Dropsit, Pat., WO2020002076A1, 2020.
- 28 M. J. Clemente, R. M. Tejedor, P. Romero, J. Fitremann and L. Oriol, *New J. Chem.*, 2015, **39**, 4009–4019.
- 29 S. A. Holey, K. P. C. Sekhar, D. K. Swain, S. Bojja and R. R. Nayak, *ACS Biomater. Sci. Eng.*, 2022, **8**, 1103–1114.
- 30 T. Xiong, X. Li, Y. Zhou, Q. Song, R. Zhang, L. Lei and X. Li, *Acta Biomater.*, 2018, **73**, 275–284.
- 31 K. Tallo, M. Bossch, T. Pons, M. Cocera and O. Lopez, *J. Mater. Chem. B*, 2020, **8**, 161–167.
- 32 P. Chakraborty, B. Das, P. Pal, S. Datta, S. Bera and P. Dastidar, *Chem. Commun.*, 2020, **56**, 5251–5254.
- 33 J. N. Israelachvili, D. J. Mitchell and B. W. J. Ninham, *Chem. Soc., Faraday Trans.*, 1976, **2**, 1525–1568.
- 34 J. C. Stendahl, M. S. Rao, M. O. Guler and S. I. Stupp, *Adv. Funct. Mater.*, 2006, **16**, 499–508.
- 35 H. Jiang, M. O. Guler and S. I. Stupp, *Soft Matter*, 2007, **3**, 454–462.
- 36 G. Yang, W. Zheng, G. Tao, L. Wu, Q.-F. Zhou, Z. Kochovski, T. Ji, H. Chen, X. Li, Y. Lu, H.-M. Ding, H.-B. Yang, G. Chen and Ming Jiang, *ACS Nano*, 2019, **13**, 13474–13485.
- 37 N. Baccile, M. Selmane, P. Le Griel, S. Prévost, J. Perez, C. V. Stevens, E. Delbeke, S. Zibek, M. Guenther, W. Soetaert, I. N. A. Van Bogaert and S. Roelants, *Langmuir*, 2016, **32**, 6343–6359.
- 38 S. Liu, H. Li, J. Zhang, X. Tian and X. Li, *RSC Adv.*, 2020, **10**, 33642–33650.
- 39 J. Liu, Z. Sun, Y. Yuan, X. Tian, X. Liu, G. Duan, Y. Yang, L. Yuan, H.-C. Lin and X. Li, *ACS Appl. Mater. Interfaces*, 2016, **8**, 6917–6924.
- 40 A. Chalard, L. Vaysse, P. Joseph, L. Malaquin, S. Souleille, B. Lonetti, J.-C. Sol, I. Loubinoux and J. Fitremann, *ACS Appl. Mater. Interfaces*, 2018, **10**, 17004–17017.
- 41 Z. Yang, G. Liang, M. Ma, A. S. Abbah, W. W. Lu and B. Xu *Chem. Commun.*, 2007, **8**, 843–845.
- 42 J. Gao, J. Zhan and Z. Yang, *Adv. Mater.*, 2020, **32**, 1805798.
- 43 R. A. Pires, Y. M. Abul-Haija, D. S. Costa, R. Novoa-Carballal, R. L. Reis, R. V. Ulijn and I. Pashkuleva, *J. Am. Chem. Soc.*, 2015 **137**, 576–579.
- 44 A. Brito, P. M. Pereira, R. L. Reis, R. V. Ulijn, J. S. Lewis, R. A. Pires and I. Pashkuleva, *Nanoscale*, 2020, **12**, 19088–19092.
- 45 A. Brito, P. M. Pereira, D. S. da Costa, R. L. Reis, R. V. Ulijn, J. S. Lewis, R. A. Pires and I. Pashkuleva, *Chem. Sci.*, 2020, **11**, 3737–3744.
- 46 Z. Yang, H. Gu, D. Fu, P. Gao, J. Lam and B. Xu, *Adv. Mater.*, 2004, **16**, 1440–1444.
- 47 Z. M. Yang, K. M. Xu, Z. F. Guo, Z. H. Guo, B. Xu, *Adv. Mater.*, 2007, **19**, 3152–3156.
- 48 J. Baillet, A. Gaubert, J. Verget, L. Latxague and P. Barthélémy, *Soft Matter*, 2020, **16**, 7648–7651.
- 49 R. Yoshisaki, S. Kimura, M. Yokoya and M. Yamanaka, *Chem. Asian J.*, 2021, **16**, 1937–1941.

ARTICLE

50 R. Hamura, Y. Shirai, Y. Shimada, N. Saito, T. Taniyai, T. Horiuchi, N. Takada, Y. Kanegae, T. Ikegami, T. Ohashi and K. Yanga, *Cancer Sci.*, 2021, **112**, 2335–2348.